



Efficacy of Ultrasound Microbubble-HGF Complex for Treating Hepatic Fibrosis and its Relation with Perfusion Weighted Imaging

Shou-Hong Zhang^{1*}, Ying Zhang¹, Kun-Ming Wen², Wei Wu³ and Wen-Yan Li³

¹Department of Nuclear Medicine, The Second Affiliated Hospital, Zhejiang University School of Medicine, Hangzhou 310000, Zhejiang, China

²Department of Gastrointestinal Surgery, Affiliated Hospital of Zunyi Medical College, Zunyi 563000, Guizhou, China

³Institute of Ultrasound Imaging, The Second Affiliated Hospital of Chongqing Medical University, Chongqing 404100, China

ABSTRACT

We explored the feasibility of treating liver fibrosis with human Hepatocyte Growth Factor (HGF) carried by biotinylated ultrasound microbubbles plus biotinylated cationic nano-liposome composites (Bio-MB+Bio-CNLP) in bile duct-ligated (BDL) rats. In addition, we investigated the staging of hepatic fibrosis by using Perfusion-Weighted Imaging (PWI). We established a BDL rat model of hepatic fibrosis. HGF carrier was administered through tail-vein injections. The gene therapy efficacy was evaluated *in vivo*. Before and after treatment the rats were examined with MR-PWI. The perfusion parameters of PWI were compared with the fibrosis stage. The total fibrous tissue in the liver of rats treated with HGF was lower than that in control group. The time-signal intensity curve (TIC) peak of liver parenchyma of rats with hepatic fibrosis was characterized by a slow wash-in-out. A correlation was found between the perfusion parameters and the stage of fibrosis. As the stage of fibrosis increased, the wash-in and -out rates decreased progressively. The use of Bio-MB+Bio-CNLP is an effective and novel vector for gene delivery *in vivo*. Further, we confirm that HGF represents a valid liver anti-fibrotic molecule. PWI might be an effective method for quantifying the severity of liver fibrosis.

Article Information

Received 12 November 2018

Revised 22 June 2019

Accepted 01 October 2019

Available online 13 November 2019

Authors' Contribution

SZ designed the study, performed experimental work and analyzed the data. YZ and KW helped in establishing the animal model. WW helped in MRI examinations. WL wrote the article.

Key words

Extra-cellular matrix, Gene therapy, Biotinylation, Expression vector, Functional imaging

INTRODUCTION

Liver fibrosis, and its ultimate stage cirrhosis, is a common process in the pathological development of a variety of chronic liver diseases (Friedman, 2003). Although cirrhosis is usually not reversible, non-cirrhotic liver fibrosis can be reversed under certain circumstances. Over-activation of hepatic stellate cells (HSC) has been shown to contribute to liver fibrosis (Chen *et al.*, 2012; Moreira, 2007). The HSC form scar tissue in response to liver damage during liver fibrosis (Ozeki *et al.*, 2012). Previous studies showed HGF an anti-fibrosis cell growth factor, can induce apoptosis in activated HSC, reduce excessive collagen deposition (Suarez-Causado *et al.*, 2015; Yu *et al.*, 2013; Campana and Iredale, 2017; Wang *et al.*, 2009), stimulate hepatocyte regeneration to promote the recovery of liver function. Gene therapy was originally proposed 45 years ago, but it is only during the last 5-10 years that significant clinical benefit has been

demonstrated (Almeer *et al.*, 2018). Thus, using HGF in gene therapy against liver fibrosis is an attractive approach. However, the current problems facing viral vectors (*e.g.* liver toxicity, immunogenicity, inflammation, low tissue specificity, complex preparation and high cost) are major barriers to the clinical application of gene therapy. Cationic liposomes have some advantages as drug, antigen and gene delivery carriers (Crespo *et al.*, 2012; Negishi *et al.*, 2013), but is plagued by low targeting and low transfection efficiency *in vivo*. Ultrasound-targeted microbubble destruction is a new non-invasive gene therapy technique, which can significantly increase gene transfection efficiency and provides an alternative approach for gene therapy of liver fibrosis (Kopechek *et al.*, 2015). However, the amount of gene vector loaded into the ultrasound microbubble is limited, and the exposed gene vector is less stable *in vivo* (Jiang *et al.*, 2013; Inaba and Lindner, 2012; Carson *et al.*, 2012; Kiessling *et al.*, 2012). In order to overcome these limitations, we aimed at combining the advantages of the above two methods.

Individualized treatment increasingly requires accurate evaluation of liver fibrosis. Lack of simple, accurate and repeatable methods to evaluate liver fibrosis

* Corresponding author: 874645@zju.edu.cn
0030-9923/2020/0001-0363 \$ 9.00/0
Copyright 2020 Zoological Society of Pakistan

has become an obstacle to clinical treatment and research of liver diseases. Liver biopsy is considered as the gold standard for the diagnosis of liver fibrosis (Sands *et al.*, 2015). Recent research shows that liver biopsy also has drawbacks, including variability, high price, sample error, too subjective observer, etc (Huang *et al.*, 2017; Friedman *et al.*, 2003; Poynard *et al.*, 2012). In order to avoid the disadvantages brought about by liver biopsy, a non-invasive Method is needed to quantitatively analyse fibrosis and its stages (Castera *et al.*, 2010). MR-PWI is a method by using dynamic susceptibility contrast-enhanced technique for evaluating the anatomic characteristics of various organs (Hagiwara *et al.*, 2008). We prospectively evaluated the sensitivity and specificity of PWI using a 3.0-T Magnetic Resonance (MR) for the diagnosis of liver fibrosis.

MATERIALS AND METHODS

Construction of HGF expression vector

The HGF gene was amplified by PCR, with pre-designed upstream and downstream primers according to the Genebank gene pool of HGF cDNA sequence. The PCR conditions were as follows: 95°C denaturation for 3 min, 95°C denaturation 10 sec, annealing at 55°C for 15 sec, and extension at 72°C for 2.5 min, 30 cycles; 72°C extensions for 10 min. PCR fragments were purified and inserted to a pCDH-EF1-MCS-T2A-copGFP vector. After transformation into *E. coli*, candidate gene clones were cultured and identified by PCR. The identified positive clone were sequenced (Sangon, Shanghai) and identified as pCDH-HGF. High amounts of purified pCDH-HGF plasmid were prepared by toxin-free plasmid extraction kit (TaKaRa Company, Japan) and stored at -20°C after determination of the plasmid concentration. Bio-MB+Bio-CNLP (The vector is done in our laboratory) was carefully mixed with pCDH-HGF plasmid, incubated for 30 min, with the final concentration of plasmid DNA at 0.01 mg/ml.

Cell transfection and protein expression detection

HGF expression were evaluated in the hepatic stellate cell line HSC-T6 (ATCC, USA). The cell lines were cultured in Dulbecco's Modified Eagle Medium (DMEM), high glucose medium containing 10% fetal bovine serum, at 37°C, in 5% CO₂ and standard conditions. The cells were passaged 2-3 times to achieve sufficient growth rate. 2.0×10^5 HSC-T6 cells were seeded to each well of six-well plates and cultured for 24h until 60-70% confluence. Before transfection, culture media were replaced by non-FBS (fetal bovine serum) DMEM. The transfection was conducted using an ultrasound gene transfection therapy instrument with S4 transducer, and a focus depth of 1-2cm. The ultrasonic parameters were: 1 MHz and 0.5 W/cm².

Each irradiation cycle was 10s in duration, separated by a 10s interval, and repeated 6 times, 4h after transfection, the culture media were replaced by fresh DMEM containing 10% FBS. After transfection by ultrasound mediated gene delivery, we examined the HGF expression in HSC-T6 cells using IF-IC and by Western blot.

Construction of the animal model and MR-PWI scanning

The bile duct ligation (BDL) experimental model was performed as described previously (Ezure *et al.*, 2000). Rats were randomly assigned in two groups: a) control group (n=23) and b) therapy group (n=39). In the therapy group, the rats were administered HGF plasmid through tail-vein injections at a concentration of 0.05µg/g every week. At the same time, ultrasound (frequency: 300KHz; intensity: 2W/cm²; time: 10s interval 10s) was exposed to the liver area. In the control group, saline was injected through tail vein at a dose of 100 ml/kg. 4 weeks later, they were sacrificed immediately after PWI scanning. Liver tissues were collected for pathological examination and hydroxyproline content detection. (All experiments were performed in accordance with the guidelines for animal research established by the Local Ethics Committee of Animal Experiments at Zhejiang University).

All MR examinations were performed on 3.0T double gradient superconducting magnetic resonance instrument (GE Signa Twinspeed) and 5.0 surface coil. Rats were prone and fixed on the scanner and the liver was placed in the center of the coil. Routine axial T1WI plain scan, TSE sequence axial T2WI, SPAIR perfusion scan, perfusion scanning parameters: excitation times: 1, TR/TE=1200ms/40ms, matrix: 119×192; FOV: 75×55mm, layer thickness: 3.0mm; interval: 0mm; region of interest (ROI) analyses, enabled the generation of time-signal intensity curve (TIC). Perfusion parameters were recorded as follows: a) time to peak (TTP); b) mean transit time (MTT); c) wash-in rate and d) wash-out rate. The correlation between perfusion parameters of PWI and stages of hepatic fibrosis was evaluated.

Hydroxyproline content

Tissue was homogenized with dH₂O and added 100 ml dH₂O per 10mg tissue. In a sealed tetrafluoroethylene bottle, 100ml of concentrated hydrochloric acid was added to the sample and hydrolyzed at 120°C for 3 hs. 96 orifice plates were vacuum dried with 10ml sample per orifice. 100ml for each sample and standard. Chloramine T was incubated at room temperature for 5 min. 100 ml DMAB was added to each pore and incubated at 60°C for 90 min. Absorption was measured at 560 nm.

Histopathological analysis

The rats were sacrificed after MR scanning immediately,

liver was removed and fixed with 10% formaldehyde. Samples corresponded to ROI in MR examination. Liver tissues were stained by hematoxylin and Masson's method. The degree of hepatic fibrosis was quantitatively analyzed by computerized morphometry. The area of hepatic fibrosis was detected by morphometric analysis software. The stages of hepatic fibrosis were: S0: no hepatic fibrosis; S1: fibrosis in portal area and local perisinusoidal fibrosis; S2: formation of fibrous septa in hepatic lobules; S3: A large number of fibrous septal formation with structural damage in hepatic lobules, but no cirrhosis; S4: early cirrhosis.

Statistical analysis

All data was processed by SPSS 13.0. Statistical software. All research data was expressed as a mean standard deviation, the correlation between perfusion parameters of MR-PWI and stages of liver fibrosis were analyzed by Spearman's correlation analysis. $P < 0.05$: statistical difference; $P < 0.01$: Significant statistical difference. The perfusion parameters of MR-PWI were taken as the analysis index. Pathological stage $S \geq 1$ is considered to be diagnostic standards of liver fibrosis and $S=4$ is considered to be diagnostic standards of early cirrhosis. The correlation between PWI perfusion parameters and different stages of liver fibrosis was analyzed, and the sensitivity and specificity of each index were calculated.

HGF expression level by Bio-MB + Bio-CNLP delivery

The HGF gene ORF fragment was generated by PCR amplification and a ~2200 bp DNA fragment was identified by agarose gel electrophoresis (Fig. 1A). After extraction and purification, the HGF cDNA was cloned into a pCDH-EF1-MCS-T2A-copGFP vector, ensuring the simultaneous expression of both HGF and GFP. We examined the HGF expression in HSC-T6. The results showed that HGF was well-expressed in the cell lines (Fig. 1B, C).

Hydroxyproline content

Determination of hydroxyproline in liver tissue showed that hydroxyproline in HGF group was significantly lower than that in control group (control group: $0.78 \pm 0.04 \mu\text{g}/\mu\text{L}$, $1.57 \pm 0.03 \mu\text{g}/\mu\text{L}$; therapy group: $0.49 \pm 0.08 \mu\text{g}/\mu\text{L}$, $0.32 \pm 0.06 \mu\text{g}/\mu\text{L}$, $P < 0.05$). The content of hydroxyproline decreased gradually after 2 and 4 weeks of treatment but increased significantly in the control group (Fig. 2).

Histopathological analysis

Histochemical stain (HE and masson) was used to check and define the pathological stage of fibrosis of the specimen tissue. With the prolongation of biliary obstruction time, the fibrous tissue around the bile duct in the control group increased, and infiltrated into the hepatic

parenchyma, which was equivalent to the stage of hepatic fibrosis S3-S4. In the HGF treatment group, the decrease of fibrous tissue was mainly confined to the periphery of bile duct, with a small area and no fibrous tissue between liver parenchyma, which was equivalent to the stage of hepatic fibrosis S1-S2 (Fig. 3a, b).

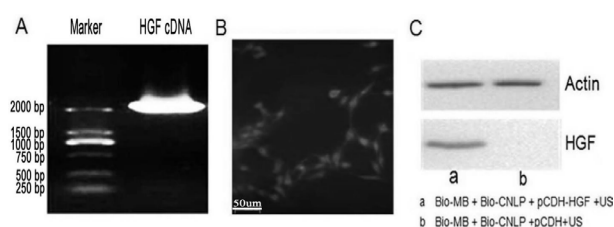


Fig. 1. The construction of HGF expression vector and preparation of Bio-MB+Bio-CNLP. The HGF cDNAs were generated by PCR amplification and the expected ~2200 bp bands are shown (A), After transfection, the HGF expression was examined (B), in HSC-T6 by IF-IC and in L02 by Western blot (C). As a negative control, L02 cells transfected with blank pCDH vector had no detectable HGF bands.

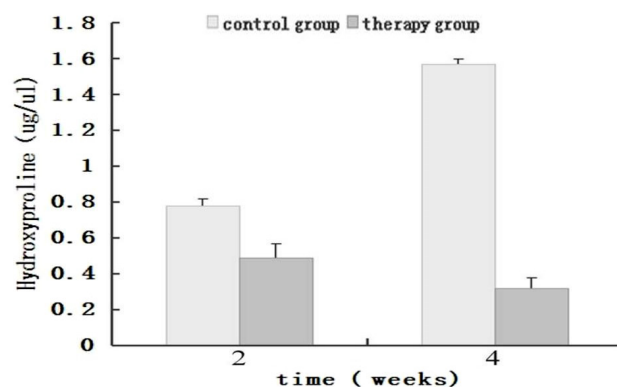


Fig. 2. Hydroxyproline Content.

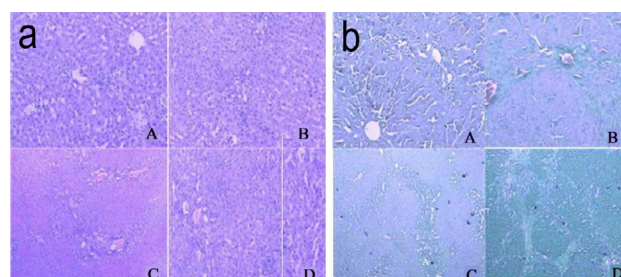


Fig. 3. a. Hematoxylin/Eosin staining of liver tissue. A) stage 1 of liver fibrosis; B) stage 2 of liver fibrosis; C) stage 3 of liver fibrosis; D) stage 4 of liver fibrosis; b. Masson's trichrome staining of hepatic tissues. A) stage 1 of liver fibrosis; B) stage 2 of liver fibrosis; C) stage 3 of liver fibrosis; D) stage 4 of liver fibrosis.

MR- PWI

After BDL, the livers of rats were examined by MRI-PWI (Fig. 4). Table I reports the comparison between the perfusion parameters of MRI-PWI and the stage of liver fibrosis (Table I), while Figure 5 shows the TIC analysis: a. TIC analysis of S0 stage hepatic fibrosis. The red line represents the perfusion curve of the abdominal aorta; the green line represents perfusion curve of the portal vein; and the blue line represents perfusion curve of the liver parenchyma; b. TIC analysis of S4 stage hepatic fibrosis. The red line represents the perfusion curve of the abdominal aorta; the blue line represents perfusion curve of the portal vein; and the green line represents perfusion curve of the liver parenchyma. The curve of the therapy group descended quickly, and then recovered slowly after peak value. The recovery extent was larger and the recovery course was shorter. The curve of the control group descended slowly, the extent of descent was smaller, the time to peak was longer, the recovery extent after peak value was smaller, the recovery course was longer, and the peak was width. With the development of hepatic fibrosis, the changes were more evident (Fig. 5).

Table I. Comparison among the PWI perfusion parameters and the stage of liver fibrosis.

Liver fibrosis (Stage)	MTT	TTP
S0	21.02±6.51	16.15±3.91
S1	25.98±3.05	18.71±2.39
S2	29.59±2.17	22.31±7.03
S3	37.26±4.81	39.21±3.37
S4	38.22±4.25	41.16±5.48

MTT, Mean transit time; TTP, Time to peak.

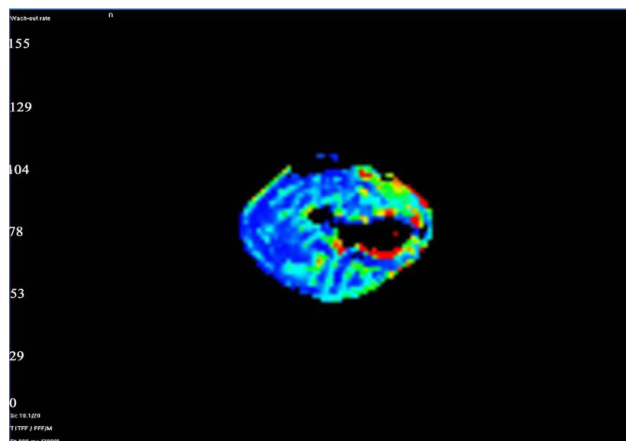


Fig. 4. The liver of rats underwent bile duct ligation (BDL) were examined by MR-PWI.

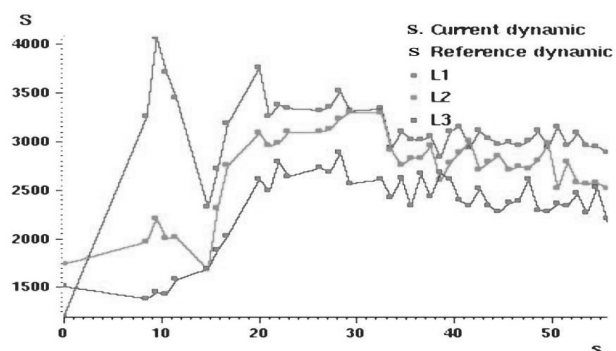


Fig. 5. Time-signal intensity curve (TIC) of hepatic fibrosis. a. TIC analysis of S0 stage hepatic fibrosis. The red line represents the perfusion curve of the abdominal aorta; the green line represents perfusion curve of the portal vein; and the blue line represents perfusion curve of the liver parenchyma. b. TIC analysis of S4 stage hepatic fibrosis. The red line represents the perfusion curve of the abdominal aorta; the blue line represents perfusion curve of the portal vein; and the green line represents perfusion curve of the liver parenchyma.

DISCUSSION

Microbubble agents can be used as delivery gene carriers in combination with ultrasound. Recent results have shown that ultrasound-targeted microbubble destruction, through mechanical cavitation effects, can increase membrane permeability, while shock waves generated by microbubble rupture provide a driving force for the gene vector to be released from the microbubble and transported into target cells (Shen *et al.*, 2009; Sirsi and Borden, 2012; Tlaxca *et al.*, 2013; Yang *et al.*, 2013). It has been reported that sudden death can occur immediately after the administration of microbubbles injected into vital organs (Tlaxca *et al.*, 2013). We investigated the structure of Bio-MB+Bio-CNLP and found that most were less than 2 μ m in diameter. In addition, Bio-MB+Bio-CNLP administration did not cause any deaths after injection, suggesting that Bio-MB+Bio-CNLP is safe when applied *in vivo*. Constructing targeted ultrasound microbubbles through the biotin-avidin connection method offers the following advantages: (1) quick connection of all new ligands on the microbubble; (2) great improvement of the signal intensity and detection sensitivity; The results of the present study confirmed that Bio-MB+Bio-CNLP, as a modified safe targeted gene transfer vector, can significantly improve the efficiency of gene transfection. HGF expression and regulatory effects were significantly enhanced with this modified system in hepatic stellate cells.

MR-PWI provides sequential whole liver imaging without radiation, a linear relationship between signal

intensity (SI) and (Gadolinium concentration) [Gd] can be assumed for the range of expected concentrations in the liver and blood. Details of the model have been described in previous studies (Quan *et al*, 2006). In this study, we performed a prospective study assessing several liver perfusion parameters, and found that the values of TTP were significantly different between S0-S1 and S2-S4, and S2 and S4 ($P<0.05$). In addition, the values of MTT were significantly different between S0 and S2-S4, and S1 and S3-S4 ($P<0.05$). According to the wash-in and wash-out rates of portal vein and liver parenchyma, S0-S1 could be distinguished from S3-S4, and S2 could be distinguished from S4 ($P<0.05$). The analysis of perfusion parameters was helpful for staging hepatic fibrosis ($P<0.001$).

CONCLUSIONS

The combination of Bio-MB+Bio-CNLP and ultrasound exposure is an effective and novel delivery gene method *in vivo*, and when properly targeted, HGF ameliorates hepatic biliary fibrosis. Furthermore, PWI could be an effective method to quantify the severity of liver fibrosis. The analysis of perfusion parameters may be helpful for staging hepatic fibrosis.

ACKNOWLEDGEMENT

We acknowledge the financial supports of the National Natural Science Foundation of China (81501508) and the Natural Science Foundation of Zhejiang Province (LQ14H180003)

Statement of conflict of interest

We declare no conflicts of interest in this study.

REFERENCES

- Almeer, R., Alqarni, A., Alqattan, S., Abdi, S., Alarifi, S., Hassan, Z. and Semlali, A., 2018. Effect of honey in improving breast cancer treatment and gene expression modulation of MMPs and TIMPs in triple-negative breast cancer cells. *Pakistan J. Zool.*, **50**: 1999-2007. <http://dx.doi.org/10.17582/journal.pjz/2018.50.6.1999.200>
- Campana, L. and Iredale, J.P., 2017. Regression of liver fibrosis. *Semin. Liver Dis.*, **37**: 1-10. <https://doi.org/10.1055/s-0036-1597816>
- Carson, A.R., McTiernan, C.F., Lavery, L., Grata, M., Leng, X. and Wang, J., 2012. Ultrasound targeted microbubble destruction to deliver siRNA cancer therapy. *Cancer Res.*, **72**: 6191-6199. <https://doi.org/10.1158/0008-5472.CAN-11-4079>
- Crespo, G., Fernández-Varo, G., Marino, Z., Casals, G., Miquel, R. and Martínez, S.M., 2012. ARFI, FibroScan®, ELF and their combinations in the assessment of liver fibrosis: A prospective study. *J. Hepatol.*, **57**: 281-287. <https://doi.org/10.1016/j.jhep.2012.03.016>
- Chen, L., Zhang, W., Zhou, Q.D., Yang, H.Q., Liang, H.F., Zhang, B.X., Long, X. and Chen, X.P., 2012. HSCs play a distinct role in different phases of oval cell-mediated liver regeneration. *Cell Biochem. Funct.*, **30**: 588-596. <https://doi.org/10.1002/cbf.2838>
- Castera, L., Sebastiani, G., Le Bail, B., de Lédinghen, V., Couzigou, P. and Alberti, A., 2010. Prospective comparison of two algorithms combining non-invasive methods for staging liver fibrosis in chronic hepatitis C. *J. Hepatol.*, **52**: 191-198. <https://doi.org/10.1016/j.jhep.2009.11.008>
- Ezure, T., Sakamoto, T., Tsuji, H., Lunz, J.G., Murase, N. and Fung, J.J., 2000. The development and compensation of biliary cirrhosis in interleukin-6-deficient mice. *Am. J. Pathol.*, **156**: 1627-1639. [https://doi.org/10.1016/S0002-9440\(10\)65034-1](https://doi.org/10.1016/S0002-9440(10)65034-1)
- Friedman, S.L., 2003. Liver fibrosis—from bench to bedside. *J. Hepatol.*, **38**: S38-S53. [https://doi.org/10.1016/S0168-8278\(02\)00429-4](https://doi.org/10.1016/S0168-8278(02)00429-4)
- Huang, Y., Deng, X. and Liang, J., 2017. Modulation of hepatic stellate cells and reversibility of hepatic fibrosis. *Exp. Cell Res.*, **352**: 420-426. <https://doi.org/10.1016/j.yexcr.2017.02.038>
- Holdsworth, S.J. and Bammer, R., 2008. Magnetic resonance imaging techniques: fMRI, DWI, and PWI. *Sem. Neurol.*, **28**: 395-406. <https://doi.org/10.1055/s-0028-1083697>
- Hagiwara, M., Rusinek, H., Lee, V.S., Losada, M., Bannan, M.A. and Krinsky, G.A., 2008. Advanced liver fibrosis: Diagnosis with 3D whole-liver perfusion MR imaging—initial experience. *Radiology*, **246**: 926-934. <https://doi.org/10.1148/radiol.2463070077>
- Inaba, Y. and Lindner, J.R., 2012. Molecular imaging of disease with targeted contrast ultrasound imaging. *Transl. Res.*, **159**: 140-148. <https://doi.org/10.1016/j.trsl.2011.12.001>
- Jiang, Z.Z., Xia, G.Y., Zhang, Y., Dong, L., He, B.Z. and Sun, J.G., 2013. Attenuation of hepatic fibrosis through ultrasound microbubble mediated HGF gene transfer in rats. *Clin. Imaging*, **37**: 104-110. <https://doi.org/10.1016/j.clinimag.2012.02.017>
- Kiessling, F., Fokong, S., Koczera, P., Lederle, W. and Lammers, T., 2012. Ultrasound microbubbles for molecular diagnosis, therapy, and theranostics. *J.*

- Nucl. Med.*, **53**: 345–348. <https://doi.org/10.2967/jnumed.111.099754>
- Kopechek, J.A., Carson, A.R., McTiernan, C.F., Chen, X., Hasjim, B. and Lavery, L., 2015. Ultrasound targeted microbubble destruction-mediated delivery of a transcription factor decoy inhibits STAT3 signaling and tumor growth. *Theranostics*, **5**: 1378–1387. <https://doi.org/10.7150/thno.12822>
- Moreira, R.K., 2007. Hepatic stellate cells and liver fibrosis. *Arch. Pathol. Lab. Med.*, **131**: 1728–1734.
- Negishi, Y., Tsunoda, Y., Hamano, N., Omata, D., Endo-Takahashi, Y. and Suzuki, R., 2013. Ultrasound-mediated gene delivery systems by AG73-modified bubble liposomes. *Biopolymers*, **100**: 402–407. <https://doi.org/10.1002/bip.22246>
- Ozeki, R., Kakinuma, S., Asahina, K., Shimizu-Saito, K. and Arai, S., 2012. Hepatic stellate cells mediate differentiation of dendritic cells from monocytes. *J. Med. Dent. Sci.* **59**: 43–52.
- Poynard, T., de Ledinghen, V., Zarski, J.P., Stanciu, C., Munteanu, M. and Vergniol, J., 2012. Performances of Elasto-FibroTest®, a combination between FibroTest® and liver stiffness measurements for assessing the stage of liver fibrosis in patients with chronic hepatitis C. *Clin. Res. Hepatol. Gastroenterol.*, **36**: 455–463. <https://doi.org/10.1016/j.clinre.2012.08.002>
- Quan, X.Y., Zhang, X.L., Sun, X.J., Xing, H.F. and Liang, W., 2006. Quantitative study of dynamic magnetic resonance perfusion-weighted imaging in rabbit models of implanted hepatic VX2 tumor. *Nan Fang Yi Ke Da Xue Xue Bao*, **26**: 620–622.
- Suarez-Causado, A., Caballero-Díaz, D., Bertrán, E., Roncero, C., Addante, A., García-Álvarez, M., Fernández, M., Herrera, B., Porrás, A., Fabregat, I. and Sánchez, A., 2015. HGF/c-Met signaling promotes liver progenitor cell migration and invasion by an epithelial-mesenchymal transition-independent, phosphatidylinositol-3 kinase-dependent pathway in an in vitro model. *Biochim. biophys. Acta*, **1853**: 2453–2463. <https://doi.org/10.1016/j.bbamcr.2015.05.017>
- Shen, Y.Y., Gao, Z.G. and Rapoport, N., 2009. Recent advances in the applications of ultrasonic microbubbles as gene or drug vectors. *Acta Pharm. Sin.*, **44**: 961–966.
- Sands, C.J., Guha, I.N., Kyriakides, M., Wright, M., Beckonert, O., Holmes, E., Rosenberg, W.M. and Coen, M., 2015. Metabolic phenotyping for enhanced mechanistic stratification of chronic hepatitis C-induced liver fibrosis. *Am. J. Gastroenterol.*, **110**: 159–169. <https://doi.org/10.1038/ajg.2014.370>
- Sirsi, S.R. and Borden, M.A., 2012. Advances in ultrasound mediated gene therapy using microbubble contrast agents. *Theranostics*, **2**: 1208–1222. <https://doi.org/10.7150/thno.4306>
- Tlaxca, J.L., Rychak, J.J., Ernst, P.B., Konkalmatt, P.R., Shevchenko, T.I. and Pizzaro, T.T., 2013. Ultrasound-based molecular imaging and specific gene delivery to mesenteric vasculature by endothelial adhesion molecule targeted microbubbles in a mouse model of Crohn's disease. *J. Control Release*, **165**: 216–225. <https://doi.org/10.1016/j.jconrel.2012.10.021>
- Wang, Z.X., Wang, Z.G., Ran, H.T., Ren, J.L., Zhang, Y. and Li, Q., 2009. The treatment of liver fibrosis induced by hepatocyte growth factor directed ultrasound-targeted microbubble destruction in rats. *Clin. Imaging*, **33**: 454–461. <https://doi.org/10.1016/j.clinimag.2009.07.001>
- Yang, D., Gao, Y.H., Tan, K.B., Zuo, Z.X., Yang, W.X. and Hua, X., 2013. Inhibition of hepatic fibrosis with artificial microRNA using ultrasound and cationic liposome-bearing microbubbles. *Gene Ther.*, **20**: 1140–1148. <https://doi.org/10.1038/gt.2013.41>
- Yu, G., Jing, Y., Kou, F., Ye, F. and Gao, L., 2013. Hepatic stellate cells secreted hepatocyte growth factor contributes to the chemoresistance of hepatocellular carcinoma. *PLoS One*, **8**: e73312. <https://doi.org/10.1371/journal.pone.0073312>